

# Physicochemical characterization of meloxicam–mannitol binary systems

Parya Reisi Nassab<sup>a</sup>, Róbert Rajkó<sup>b</sup>, Piroska Szabó-Révész<sup>a,\*</sup>

<sup>a</sup> Department of Pharmaceutical Technology, University of Szeged, Eötvös u.6., H-6720 Szeged, Hungary

<sup>b</sup> Department of Unit Operations and Environmental Engineering, University of Szeged, Moszkvai krt. 5-7, H-6725 Szeged, Hungary

Received 2 December 2005; received in revised form 24 February 2006; accepted 28 February 2006

Available online 18 April 2006

## Abstract

The dissolution behaviour of drugs remains one of the most challenging aspects in formulation development. The anti-inflammatory drug, meloxicam (ME) has poor water solubility. The object of this experiment was to improve the rate of dissolution of meloxicam in capsule form. In order to achieve this, mannitol was used as a carrier in different ratios, in physical mixtures and melted forms. Mannitol, a sugar alcohol, is a cheap and readily available excipient. Differential scanning calorimetry (DSC) and X-ray diffractometry were used to investigate the characteristics of meloxicam–mannitol binary systems. Multivariate curve resolution (MCR) as a chemometric method was applied to interpret the X-ray diffractograms. This is believed to be the first published use of this reasoning for this interpretation. According to the results, the amount of mannitol and the particle size of ME were important factors in the rate of dissolution. To the perfect dissolution of ME, the melt technology was used which resulted in mixed crystals. This technology was made by 10 parts of mannitol and 1 part of ME2 with about 6  $\mu\text{m}$  in average particle size. The interaction (adhesion) between mannitol and ME for physical mixtures was not enough to the perfect dissolution.

© 2006 Elsevier B.V. All rights reserved.

**Keywords:** Meloxicam; Mannitol; Dissolution; X-ray diffractometry; Multivariate curve resolution (MCR); Chemometrics

## 1. Introduction

Meloxicam (ME; 4-hydroxy-2-methyl-*N*-(5-methyl-2-thiazolyl)-2H-benzothiazine-3-carboxamide-1,1-dioxide) is a highly potent non-steroidal anti-inflammatory drug (NSAID) of the enolic acid class of oxamic derivatives. ME is a potent inhibitor of cyclooxygenase (COX), and in several models exhibits selectivity for the inducible isoenzyme COX2. The structure of ME is shown in Fig. 1. It is used to treat rheumatoid arthritis, osteoarthritis and other joint diseases [1,2]. Besides its main function as an anti-inflammatory drug, it is also emerging as a useful agent in Alzheimer's disease and cancer (mainly colorectal and adenocarcinoma) treatment [3–6]. Other advantages of meloxicam are:

- less irritation of gastrointestinal and local tissue (dermal, rectal and ocular) [1], although meloxicam is mainly absorbed in the duodenum (intestinal absorption) [7];
- fewer renal side-effects as compared with other NSAIDs [6,8–10].

Like many other NSAIDs, ME is practically insoluble in water. ME can be graded in Class II, of the Biopharmaceutical Classification System, which means low aqueous solubility and rapid absorption (high permeability) through the gastrointestinal tract [7]. The bioavailability of these drugs can generally be improved by formulation techniques such as the preparation of binary systems with a hydrophilic carrier by mixing, melting or solvent methods [11,12]. Naidu et al. [2] used cyclodextrins to increase the dissolution properties of ME. Coevaporated binary systems with cyclodextrins (an aqueous solution of cyclodextrin + an ammonia solution of ME) resulted in complexes with superior dissolution properties as compared with those of kneaded systems and physical mixtures.

Mannitol, a water-soluble polyol, has attracted attention as the most popular substance used in binary systems to increase the rate of dissolution of an active ingredient in a physical mixture or melted product (solid dispersion) [13]. In the preparation of a solid dispersion, the drug can be mixed in the melted excipient and, after solidification, the product is suitable for further processing. The melt technology is up-to-date “green” technology as it does not use any organic solvent. Mannitol is applicable for this purpose, because it is very stable to heat and melts without decomposition [14].

\* Corresponding author. Tel.: +36 62 545572; fax: +36 62 545571.  
E-mail address: [revesz@pharm.u-szeged.hu](mailto:revesz@pharm.u-szeged.hu) (P. Szabó-Révész).

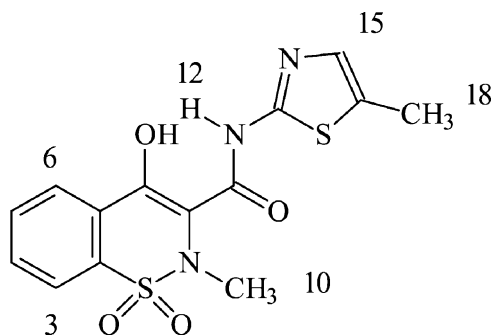


Fig. 1. Structure of meloxicam [2].

In this work,  $\beta$ -D-mannitol was used in an attempt to increase the rate of dissolution of the poorly soluble ME. We studied the dissolution properties of MEs with different particle sizes, in the ME–mannitol binary system to clarify how the rate of dissolution of ME is influenced:

- by the particle size and the specific surface of the ME,
- by the amount of mannitol, and
- by the technology applied (mixing and melting).

## 2. Materials and methods

### 2.1. Materials

ME samples with different particle sizes (ME1 and ME2) were supplied by EGIS Ltd. (Budapest, Hungary).  $\beta$ -D-Mannitol was from Hungaropharma Ltd. (Budapest, Hungary). All other reagents and solvents were of analytical grade. The particle size and its specific surface of for all materials, which can be seen in Table 1, were measured by laser diffraction (Malvern Mastersizer 2000, Malvern Ltd., Worcestershire, UK). For the measurements, the materials were dispersed by air and deagglomerated with air pressure of 0.5 bar. The particle size was determined in the range 0.02–2000  $\mu\text{m}$  and the specific surfaces of the samples were calculated from the particle size data. The measurements were repeated three times.

#### 2.1.1. Preparation of solid binary systems

**2.1.1.1. Physical mixtures.** PMs of ME1 and ME2 and mannitol (ME1-PM and ME2-PM) in ratios of 3:7 (w/w) and 1:10 (w/w) were obtained by mixing the individual components for 10 min in a Turbula mixer (Turbula WAB, Systems Schatz, Switzerland) at 50 rpm.

Table 1  
Particle sizes and specific surface areas of the materials

Samples	$d$ ( $\mu\text{m}$ )			Specific surface area ( $\text{m}^2/\text{g}$ )
	10%	50%	90%	
ME1	50.50	106.66	206.20	0.071
ME2	0.72	2.49	5.97	2.514
Mannitol	17.61	86.74	239.45	0.226

**2.1.1.2. Melted products.** MPs of ME1 and ME2 and mannitol (ME1-MP and ME2-MP) in ratios of 3:7 (w/w) and 1:10 (w/w) were made as follows: the MEs were added to melted mannitol (170  $^{\circ}\text{C}$ ) and the melts solidified at room temperature (20  $\pm$  1  $^{\circ}\text{C}$ ). The products were triturated in a mortar and were sieved. The particle size range of the products was between 100 and 250  $\mu\text{m}$ .

### 2.1.2. Capsule filling

The products of MP and PM binary systems were measured by balance and filled into hard gelatine capsules (No. 2) by hand. Each one of capsules contented 15 mg of ME. (The therapeutical dose of ME is 7–15 mg.)

## 2.2. Methods

### 2.2.1. Dissolution studies

Dissolution tests were performed by using Pharmatest equipment (Hainburg, Germany), at a paddle speed of 100 rpm. Artificial enteric juice (900 ml) with a pH of 7.5 ( $\pm$ 0.1) (Ph. Eur. 4) at 37  $^{\circ}\text{C}$  ( $\pm$ 0.5  $^{\circ}\text{C}$ ) was used. The ME contents of the samples were measured spectrophotometrically at 362 nm (Helios  $\alpha$  Spectronic, Unicam, Cambridge, UK). The dissolution experiments were conducted in triplicate.

### 2.2.2. Differential scanning calorimetry (DSC)

Thermal analysis was carried out with a DSC821 $^{\circ}$  instrument (Mettler-Toledo GmbH, Switzerland). Sixteen milligrams of sample was weighed into a non-hermetically sealed aluminium pan. The samples were heated from 25 to 300  $^{\circ}\text{C}$  at a heating rate of 5  $^{\circ}\text{C}/\text{min}$ . The instrument was calibrated by using indium. All the DSC measurements were made in argon atmosphere and the flow rate was 100 ml/min. From the DSC curves, the calorimetric enthalpy,  $\Delta H$  (integral normalized value) and the peak temperature ( $T$ ) were calculated by software (Star $^{\circ}$  version 6).

### 2.2.3. Powder X-ray diffractometry (XRPD)

XRPD was performed with a Philips X-ray diffractometer (PW 1050/70 PW 1710), where the tube anode was Cu with  $K\alpha = 1.54242 \text{ \AA}$ . The pattern was collected with 50 kV of tube voltage and 40 mA of tube current in step scan mode (step size 0.035, counting time 1 s/step). The instrument was calibrated by using silicium produced by Philips. The setting error to the silicium etanol was not more than 0.01/2 $\theta$ .

### 2.2.4. Chemometric method

The method of multivariate curve resolution with alternative least squares (MCR-ALS) [15–17], as a chemometric method, can decompose the data matrix to profiles (composition profiles and pure diffractogram profiles) with the use of certain constraints [18–20]. The usual assumption in multivariate resolution methods is that the experimental data follow a bilinear model similar to the Lambert–Beer law in absorption spectroscopy. In

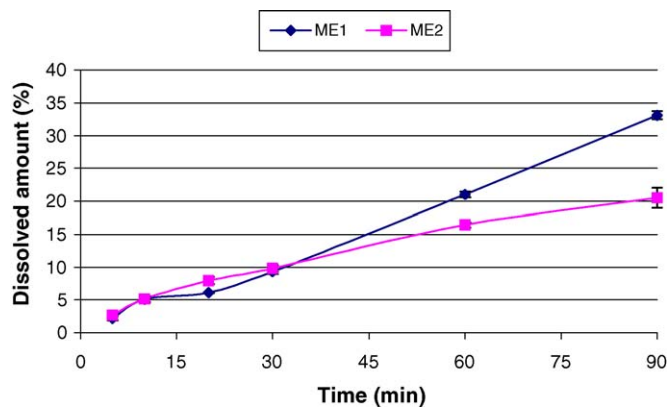


Fig. 2. Rate of dissolution and the kinetic parameters of ME1 and ME2. ME1:  $y = 0.3601x - 0.0959$  ( $k = 0.3601$ ,  $r^2 = 0.9907$ ). ME2:  $y = 0.2042x + 3.1087$  ( $k = 0.2042$ ,  $r^2 = 0.9781$ ).

matrix form, this model can be described as

$$\mathbf{R}_{I \times K} = \mathbf{D}_{I \times N} \mathbf{C}_{N \times K}^T \quad (1)$$

where  $\mathbf{R}$  is the response matrix (i.e. the counts in a diffractometry measurement against 2 theta from sample to sample),  $\mathbf{D}$  the diffractogram profile matrix of the components, and  $\mathbf{C}$  is the composition profile matrix for the samples. The matrix dimensions are indicated below the symbols of the matrices in the equations, where index  $I$  denotes the number of  $2\theta$  values,  $K$  the number of samples, and  $N$  means the number of crystalline components of the samples (mixtures) to be analysed.

Suitably chosen initial estimations of  $\mathbf{D}$  or  $\mathbf{C}$  are optimized by solving Eq. (1) iteratively by alternating least squares optimization:

$$\begin{aligned} \mathbf{D}^+ \mathbf{R}^* &= \mathbf{C}^T \\ N \times I \times K & \quad N \times K \end{aligned} \quad (2)$$

$$\mathbf{R}^* (\mathbf{C}^T)^+ = \mathbf{D}$$

$$I \times K \quad K \times N \quad I \times N$$

where the matrix  $\mathbf{R}^*$  is the reproduced data matrix obtained by principal component analysis for the selected number of com-

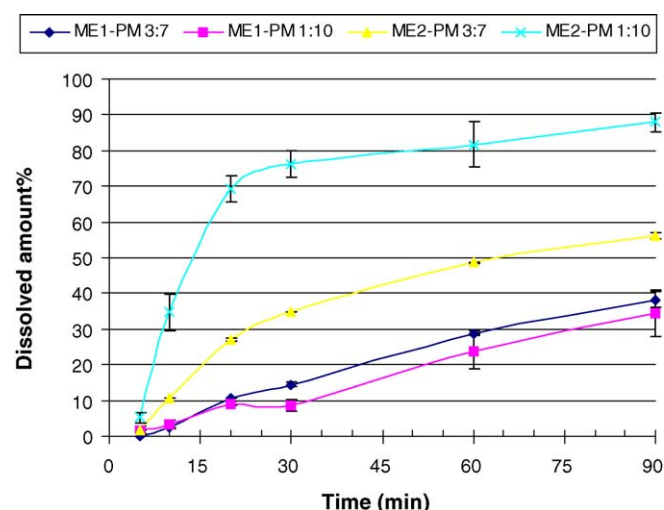


Fig. 3. Rate of dissolution of ME1-mannitol and ME2-mannitol PMs.

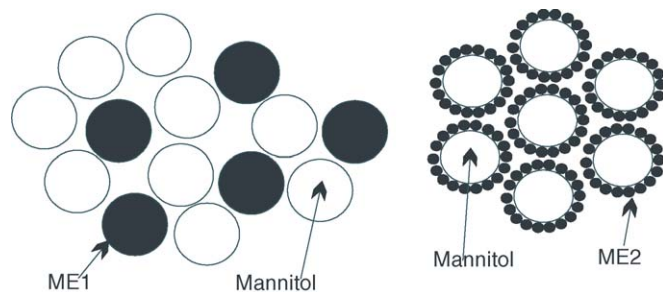


Fig. 4. Arrangement of MEs and mannitol in PMs.

ponents, and  $+$  means the pseudoinverse [21]. Unfortunately, this decomposition is very often not unique because of the rotational and intensity (scaling) ambiguities [22–23]. The rotational ambiguities can be moderated or even eliminated if convenient constraints can be used [18–20]. Tauler and coworkers developed a Matlab code for MCR-ALS with some constraints [24].

### 3. Results and discussion

#### 3.1. Particle size and specific surface area

The main possibilities for improving the dissolution of ME are to increase the surface area available for dissolution by decreasing the particle size of the drug material and by optimizing the wetting characteristics of the crystal surface [13,14]. The investigated ME1 had a particle size approximately 40 times larger than that of ME2, which was milled by Retsch PM 200 ball miller (Retsch GmbH, Haan, Germany) with 400 rpm for 40 min (Table 1).

The  $d(90\%)$  value of mannitol was nearly the same as that of ME1, but the  $d(10\%)$  value for the particles lay in the range  $\leq 17.6 \mu\text{m}$ . It follows, that mannitol had a three times larger specific surface area than that of ME1. For the development of the ratios of the components of the PMs, the starting-point was the particle sizes and the specific surface areas of the components (ME1, ME2, and mannitol). For ME1 and mannitol with same

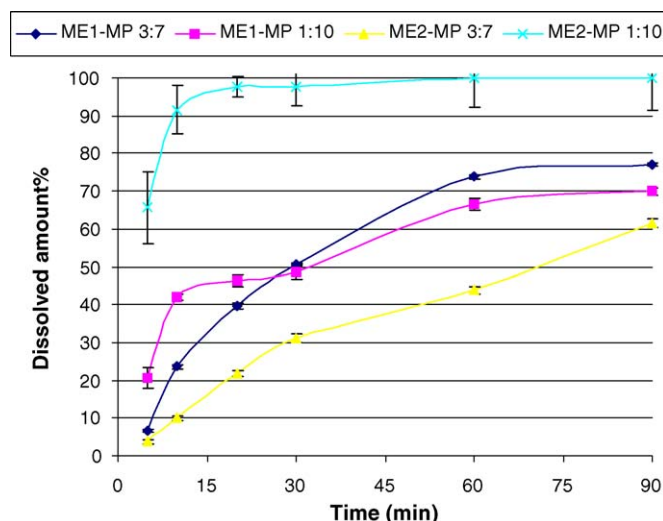


Fig. 5. Rate of dissolution of ME1-mannitol and ME2-mannitol MPs.

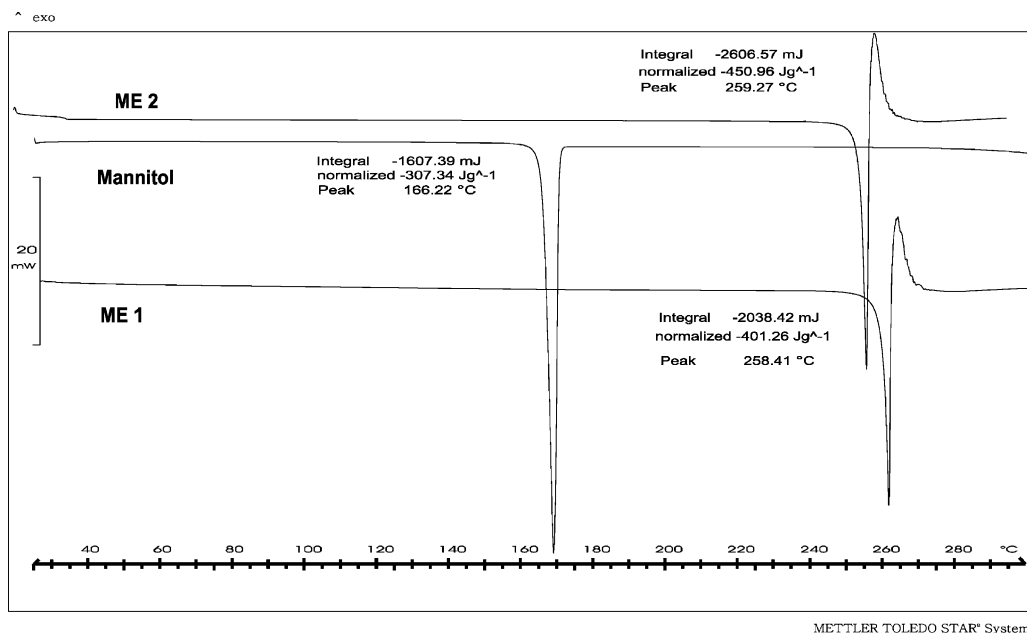


Fig. 6. DSC curves of ME1, ME2, and mannitol.

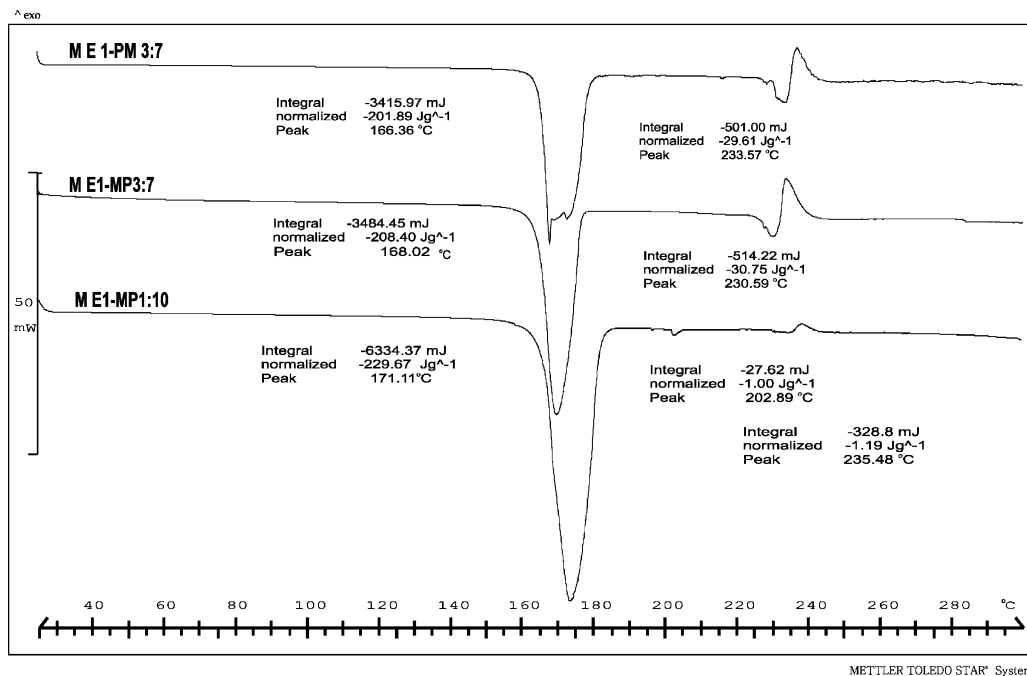
particle size, the specific surface area of mannitol was increased by increasing the amount of mannitol in the PMs (7 and 10 parts). For micronized ME2, at the previous ratios, the specific surface of ME2 was the determinative factor. The components were used in the same ratios (3:7 and 1:10) in the MPs.

### 3.2. Dissolution studies

The drug profiles of pure ME1 and ME2 were first studied (Fig. 2). The wettability of the particles was very low because the ME is a poorly water soluble drug. Difference in release

between the two drugs could be observed after 60 min. The effect of the higher specific surface area of ME2 was not manifested because of the tendency of the small ( $\sim 6 \mu\text{m}$ ) crystals to agglomerate. After dissolving of the capsule, the particles that were very hydrophobic form clustered in the artificial enteric juice. It is demonstrated by the rate constants ( $k$ ) of dissolution of MEs which were calculated according to zero kinetic order.

The effects of the particle size of the MEs and the role of mannitol were studied in the binary systems by using PMs. The dissolution rate results showed that the amount of mannitol (ratio) and its specific surface area did not influence the

Fig. 7. DSC curves of ME1-PM 3:7 and ME1-MP with ratios of 3:7 and 1:10 ( $\Delta H$  = integral normalized value, peak = temperature).

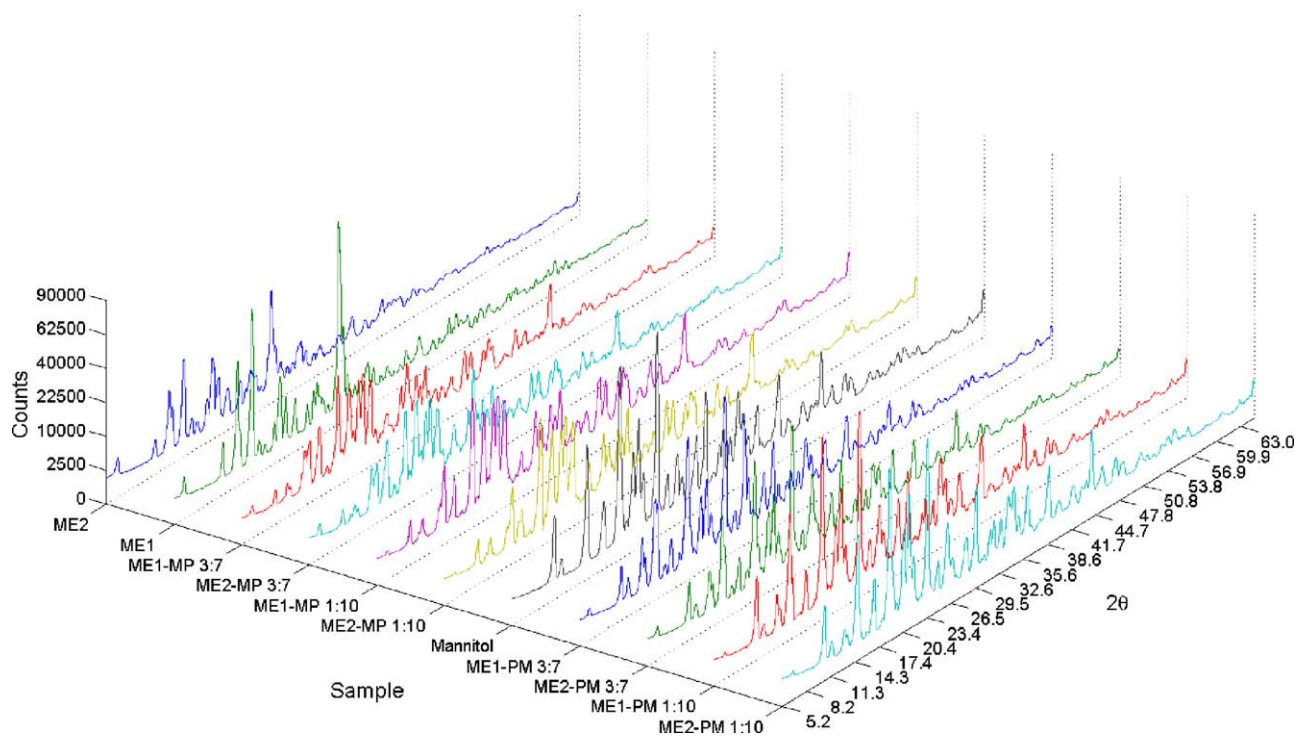


Fig. 8. X-ray diffractograms of ME1, ME2, mannitol, and ME–mannitol binary systems.

rate of dissolution of ME1 (Fig. 3). This is evidence that the ME1 and mannitol particles with same particle size only mixed together, as it shown in Fig. 4. However, in the case of ME2, on increase of the amount of mannitol (1:10), the dissolution was faster. This is connected with the specific surfaces of ME2 and mannitol. ME2 with small particles presumably adheres to the surface of mannitol (Fig. 4). Nevertheless, it should be noted that the total amount of ME2 did not dissolve.

Another possibility for the processing of ME–mannitol systems is melt technology, based on the melted mannitol as carrier containing the MEs in dispersed form. This form may be a eutectic mixture, a solid dispersion with a non-molecular distribution of the drug material or a solid solution with a molecular distribution of the drug material. Of course, the type of drug distribution influences the dissolution profile. In general, for crystalline binary systems, a molecular distribution of the drug ensures fast release. The components and their ratios in the samples prepared by melt technology were identical to those of the PMs. Fig. 5 demonstrates the influence of the melt technology on the drug release. For MP-ME1, the amount dissolved of ME1 was almost twice as much as in the case of the PMs (see Fig. 4). For the MP-ME2 samples, we achieved perfect dissolution with a higher concentration of mannitol (10 parts). The results revealed the different effects of the melt technology on the rate of dissolution of the MEs. As it was mentioned in the case of Fig. 2, although the particle size of ME2 is smaller than ME1 but the cohesion between ME2 particles is strong enough to slow down the wetting of particles by artificial enteric juice. Additionally, particle size is not the only factor, which influences the dissolution rate (that is why mannitol has been used). It seems in the case of MP-ME2 with ratio of 3:7, the amount of mannitol was

not enough to overcome this problem. For an explanation of the results, we investigated by DSC the nature of the ME dissolution in the recrystallized mannitol.

### 3.3. Differential scanning calorimetry

The DSC curves of the starting compounds exhibited a sharp endothermic peak at 165 °C, corresponding to the melting point of mannitol, and at 260 °C, the melting point of MEs (Fig. 6). The melting point of the MEs is followed by exothermic peak, which

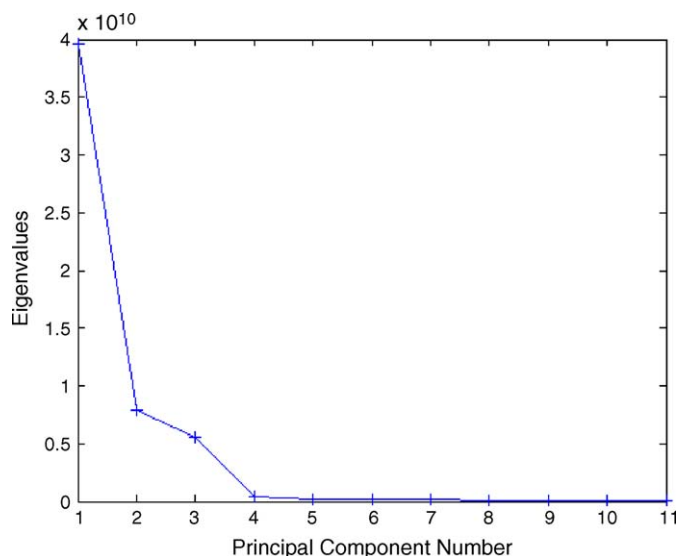


Fig. 9. Scree-plot demonstrating that three latent variables (principal components) are sufficient.

means the transformation or recrystallization of the drug material. The DSC scans of the PMs and the MPs of ME–mannitol always included two endotherms, attributed to the separate melting processes of the two components (Fig. 7). It can be seen in the DSC curve of the PM (Fig. 7) that proportion of the ME was dissolved in the melted mannitol (a broad, double endothermic peak), but the samples prepared by melting technology did not display the double peak because this dissolution might occur during the preparation of the samples. The peaks observe for the ME1 cases were analogous to those observed for ME2 at the corresponding ratios. A small additional peak is seen at a ratio of 1:10, but not at 3:7. We wanted to confirm the findings by powder X-ray investigation of the amorphous phase (the molecular distribution of ME) and the appearance of the new endothermic peak between the melting points of mannitol and ME.

### 3.4. Powder X-ray diffractometry

The results of the structural investigation of the starting materials (ME1, ME2, and mannitol), the PMs and the MPs were as follows.

The diffractograms of the PMs showed the characteristic values of the starting materials. Those of the MPs (3:7 and 1:10) had the same characteristic values as those of the PMs. The drug was distributed in the carrier in fine crystal (suspended) form. A proportion of the ME dissolved in the melted mannitol, but it was recrystallized during cooling. The remainder of the crystals were in suspended form in the binary system during the melting process. This method of drug distribution promoted drug

release, but it was not perfect. The diffractometry on the MPs containing ME1 and ME2 (1:10) showed a new peak between those of ME and mannitol, referring to the mixed crystals. Presumably these mixed crystals could be seen at 202.89 °C in the DSC curves, and this is connected with the rapid dissolution in the case of the higher amount of mannitol (10 parts). The X-ray evaluation of the binary systems raised the problem of the covered peaks (Fig. 8). To determine the differences between the X-ray diffractograms, and primarily to justify the presence of the mixed crystals, we used chemometric evaluation. This method is a new possibility for evaluation of the results of X-ray investigations. After principal component analysis, it could be concluded that 3 latent variables (principal components) were sufficient to explain 98.01% of the variations in the total data according to the scree-plot (Fig. 9).

If we know the number of components, the multivariate curve resolution method can resolve the raw data to physically interpretable factors, i.e. the composition factors of the pure components (composition profiles) and the diffractogram factors of the pure components (diffractogram profiles), using constraints of non-negativity for both profile matrices. The composition profiles show (see Fig. 10) that the solid line can be assigned to mannitol, and the dashed line to ME1, but the dotted line cannot be clearly assigned to ME2. The dotted line may represent a 'blend' of the pure components ME2, mannitol, and ME1, i.e. a new crystalline form. The 'blend' appeared in predominant amounts in the MPs, but only as a minor component in the PMs. The evaluation of the X-ray measurements with MCR confirmed the conclusions drawn from the DSC measurements:

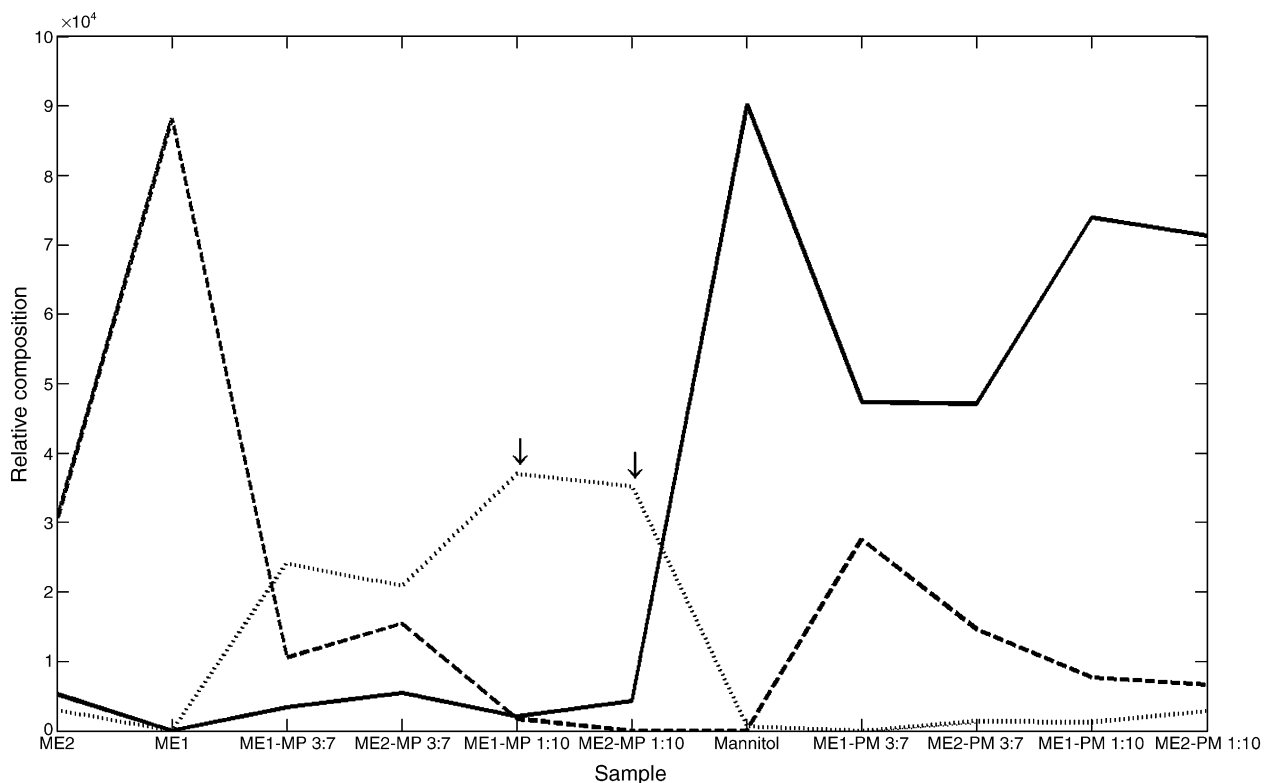


Fig. 10. Composition profiles of the three crystalline components given by MCR. Solid line: mannitol; dashed line: ME1; dotted line: 'blend'.

ME-MP 1:10 gave the highest amount of the new crystal form; the new endothermic peak (Fig. 7) appeared only at the 1:10 ratio. The PMs predominantly display the characteristics of mannitol.

#### 4. Conclusions

This study of the dissolution of meloxicam–mannitol binary systems in artificial enteric juice has revealed that both the particle size and the amount of mannitol are important factors influencing the dissolution of ME. It was shown that preparation of a PM is more useful when the ME is in micronized form ( $\mu\text{m}$ ). In the case of a MP, a high amount of mannitol (1:10) is used but even in this case the ME particle size plays an important role. Thus, the amount of mannitol and the ME particle size act in conjunction to increase the dissolution of ME.

#### Acknowledgements

The authors gratefully acknowledge the support provided for this study by the Hungarian National Research Foundation (OTKA T-047166 and T-046484) and by the János Bolyai Research Fellowship (R.R.).

#### References

- [1] P. Luger, K. Daneck, W. Engel, G. Trummlitz, K. Wagner, *Eur. J. Pharm. Sci.* 4 (1996) 175–187.
- [2] N.B. Naidu, K.P.R. Chowdary, K.V.R. Murthy, V. Satyanarayana, A.R. Hayman, G. Becket, *J. Pharm. Biomed. Anal.* 35 (2004) 75–86.
- [3] R.N. Rao, S. Meena, A.R. Rao, *J. Pharm. Biomed. Anal.* 39 (2005) 349–363.
- [4] N. Seedher, S. Bhatia, *J. Pharm. Biomed. Anal.* 39 (2005) 257–262.
- [5] A.P. Goldman, C.S. Williams, H.M. Sheng, L.W. Lamps, V.P. Williams, M. Pairet, J.D. Morrow, R.N. DuBois, *Carcinogenesis* 19 (1998) 2195–2199.
- [6] R. Banerjee, M. Sarkar, *J. Lumin.* 99 (2002) 255–263.
- [7] M. Yazdani, K. Briggs, C. Jankovsky, A. Hawi, *Pharm. Res.* 21 (2004) 293–299.
- [8] J.R. Vane, Y.S. Bakhle, R.M. Botting, *Annu. Rev. Pharmacol. Toxicol.* 38 (1998) 97–120.
- [9] G. Dannhardt, W. Kiefer, *Eur. J. Med. Chem.* 36 (2001) 109–126.
- [10] C.J. Hawkey, *Lancet* 353 (1999) 307–314.
- [11] Z. Aigner, Á. Kézsmárki, M. Kata, Cs. Novák, I. Erős, *J. Incl. Phenom.* 42 (2002) 227–233.
- [12] H.B. Hassan, M. Kata, I. Erős, Z. Aigner, *J. Incl. Phenom.* 50 (2004) 219–226.
- [13] N. Zajc, S. Srčič, *J. Therm. Anal. Cal.* 77 (2004) 571–580.
- [14] Á. Gombás, P. Szabó-Révész, G. Regdon Jr., I. Erős, *J. Therm. Anal. Cal.* 73 (2003) 615–621.
- [15] R. Tauler, E. Casassas, A. Izquierdo-Ridorsa, *Anal. Chim. Acta* 248 (1991) 447–458.
- [16] R. Tauler, *Chemom. Intell. Lab. Syst.* 30 (1995) 133–146.
- [17] A. de Juan, R. Tauler, *Anal. Chim. Acta* 500 (2003) 195–210.
- [18] A. de Juan, Y. Vander Heyden, R. Tauler, D.L. Massart, *Anal. Chim. Acta* 346 (1997) 307–318.
- [19] R. Tauler, *J. Chemom.* 15 (2001) 627–646.
- [20] M.H. Van Benthem, M.R. Keenan, D.M. Haaland, *J. Chemom.* 16 (2002) 613–622.
- [21] G.H. Golub, C.F. Van Loan, *Matrix Computations*, second ed., The John Hopkins University Press, Baltimore, 1989.
- [22] R. Tauler, A. Smilde, B.R. Kowalski, *J. Chemom.* 9 (1995) 31–58.
- [23] J.-H. Jiang, Y. Liang, Y. Ozaki, *Chemom. Intell. Lab. Syst.* 71 (2004) 1–12.
- [24] R. Tauler, A. de Juan, *Multivariate Curve Resolution Homepage*, <http://www.ub.es/gesq/mcr/mcr.htm> (latest accessed in 21 March 2005).